Accepted Manuscript

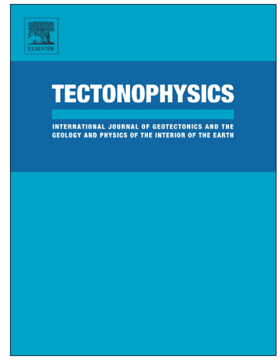

Tectonic insights of the southwest Amazon Craton from geophysical, geochemical and mineralogical data of Figueira Branca mafic-ultramafic suite, Brazil

Vinicius H.A. Louro, Peter A. Cawood, Marta S.M. Mantovani, Vanessa B. Ribeiro

PII: S0040-1951(17)30159-2
DOI: doi: 10.1016/j.tecto.2017.04.025
Reference: TECTO 127470

To appear in: *Tectonophysics*

Received date: 29 January 2017
Revised date: 19 April 2017
Accepted date: 20 April 2017

Please cite this article as: Vinicius H.A. Louro, Peter A. Cawood, Marta S.M. Mantovani, Vanessa B. Ribeiro , Tectonic insights of the southwest Amazon Craton from geophysical, geochemical and mineralogical data of Figueira Branca mafic-ultramafic suite, Brazil. The address for the corresponding author was captured as affiliation for all authors. Please check if appropriate. Tecto(2017), doi: 10.1016/j.tecto.2017.04.025

Tectonic insights of the Southwest Amazon Craton from geophysical, geochemical and mineralogical data of Figueira Branca Mafic-Ultramafic Suite, Brazil

Vinicius H. A. Louro[1,2], Peter A. Cawood[2,3], Marta S. M. Mantovani[1], Vanessa B. Ribeiro[1,4]

[1] Instituto de Astronomia, Geofísica e Ciências Atmosféricas, Universidade de São Paulo, São Paulo, Brazil.

[2] Department of Earth and Environmental Sciences, University of St. Andrews, St. Andrews, UK.

[3] School of Earth, Atmosphere & Environment, Monash University, Melbourne, VIC 3800, Australia

E-mails: vilouro@usp.br, peter.cawood@monash.edu, msmmanto@usp.br

Corresponding author: Vinicius Hector Abud Louro.

E-mail: vilouro@usp.br

Phone: +55 (11) 99985 1501

Date of Submission: 28 January 2017

Abstract

The Figueira Branca Suite is a layered mafic-ultramafic complex in the Jauru Terrane, southwest Amazon Craton. New lithological, geochemical, gamma-ray and potential field data, integrated with geological, isotope and paleomagnetic data are used to characterize this pulse of Mesoproterozoic extension-related magmatism. The Figueira Branca Suite formed through juvenile magma emplacement into the crust at 1425 Ma, coeval with the later stages of the Santa Helena Orogen. Gabbros and peridotite-gabbros display increasing enrichment of LREE, interpreted as evidence of progressive fractionation of the magma. Magnetic and gamma-ray data delimit the extent of magmatism within the suite to four bodies to the north of Indiavaí city. Modelling gravity and magnetic field data indicate that the anomalous sources are close to the surface or outcropping. These intrusions trend northwest over 8 km, with significant remanent magnetization that is consistent with published direction obtained through paleomagnetic data. The emplacement, mineralogy and geochemical signature point towards a back-arc extension tectonic framework in the later stages of the Santa Helena Orogen.

Keywords

Potential Fields; Geochemistry; Mineralogy; Radiometrics; Amazon Craton

1. *Introduction*

The Amazon Craton is divisible into six geochronological provinces: Central Amazon, including the stable Archean nuclei of the craton, and the Proterozoic provinces of Maroni-Itacaiúnas, Ventuari-Tapajós, Rio Negro-Juruena, Rondonian-San Ignácio and Sunsás-Aguapeí (Fig. 1a) (Tassinari and Macambira, 1999; Teixeira et al., 2010). The southern portion of the Rio Negro-Juruena (1.78 – 1.55 Ga) province includes the Jauru Terrane (1.78 – 1.40 Ga), which contains Paleoproterozoic basement rocks and the Mesoproterozoic Cachoeirinha and Santa Helena orogens (Fig. 1b) (Bettencourt et al., 2010). The Alto Jauru Group, part of the Paleoproterozoic basement, hosts the Figueira Branca Mafic-Ultramafic Suite, the focus of this paper.

The Figueira Branca Suite occurs in the southwest of the Mato Grosso State, Brazil, and to the southwest of the Parecis Basin (Fig. 1b). Our aim is to integrate new lithological, geochemical, gamma-ray and potential field data with available geological, isotope and paleomagnetic data to characterize the Figueira Branca Suite and delimit the extent of this Mesoproterozoic magmatic pulse.

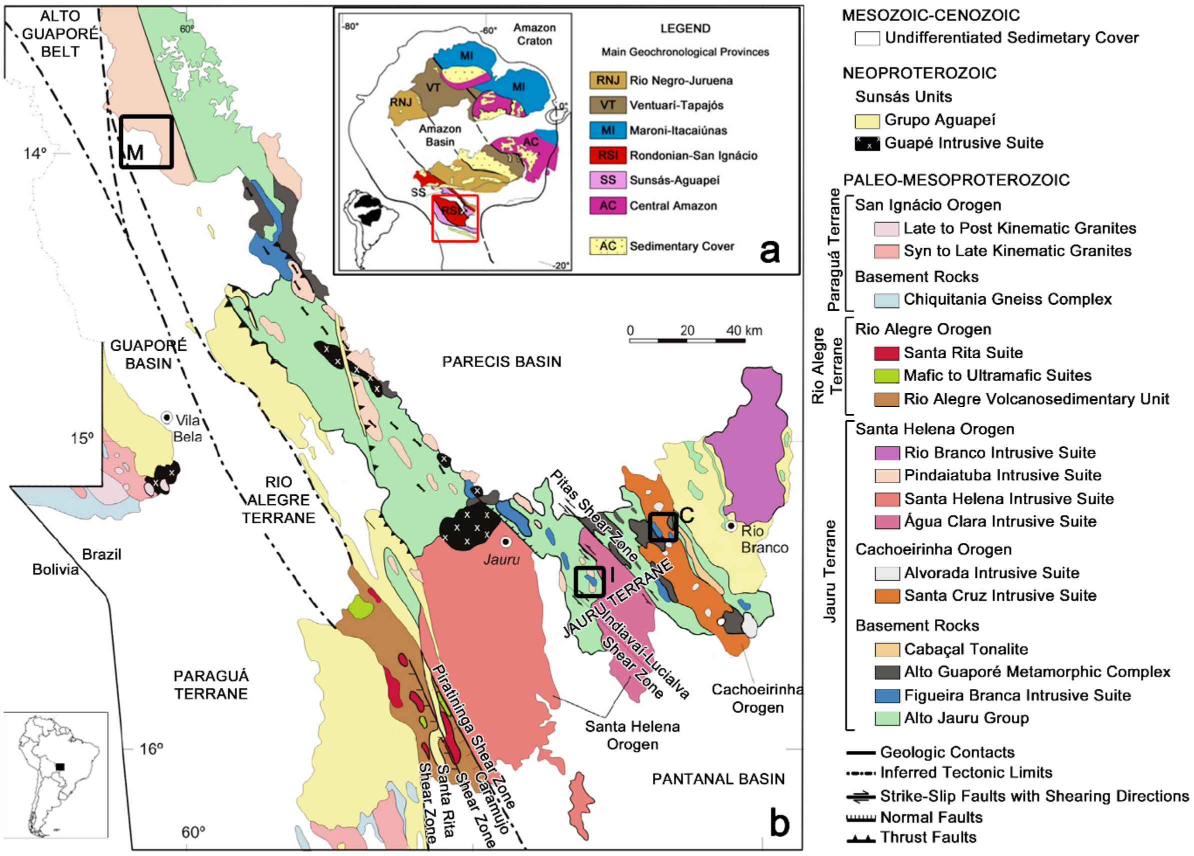

Fig. 1 – (a) Main geochronological provinces of Amazon Craton (Bettencourt et al., 2010). The red polygon delimits the area of Fig. 1b. (b) Southwest of the Rio Negro-Juruena and Rondonian-San Ignácio provinces of the Amazon Craton. The Figueira Branca Suite is represented in dark blue. The black boxes indicate the bodies near the city of Indiavaí (I) and Cachoeirinha (C) (Bettencourt et al., 2010), and the Morro do Leme and Morro do Sem-Boné mafic-ultramafic suites (M).

2. *Geologic and Tectonic Framework*

Cordani et al. (2010) use regional geochronological and tectonic patterns to propose that the development of the southwest Amazon Craton occurred within a series of accretionary orogens. This regime was responsible for the production of numerous magmatic arcs and related magmatism until the late Mesoproterozoic (Teixeira et al., 2016). The Alto Jauru Group and the Alto Guaporé Metamorphic Complex (Fig. 1b) compose the Jauru Terrane, Rio Negro-Juruena Province (Matos et al., 2009; Souza et al., 2009). The Alto Jauru Group (1760 to 1720 Ma) (Monteiro et al., 1986; (Bettencourt et al., 2010) comprises gneiss, migmatites and three meta-volcanosedimentary sequences: Cabaçal, Araputanga and Jauru. The Alto Guaporé Metamorphic Complex (1790 to 1740 Ma) (Menezes, 1993) is characterized by granodioritic to tonalitic orthogneiss intruded into supracrustal volcanosedimentary sequences, with all metamorphosed to greenschist or amphibolite facies (Bettencourt et al., 2010).

During the evolution of the Rondonian-San Ignácio Province, the Jauru Terrane underwent compressional deformation related to ocean closure, marked by the Guaporé suture and collision of the Paraguá terrane (Rizzotto et al., 2013) (Fig. 01). Subduction associated with ocean closure resulted in magmatic activity preserved in the Cachoeirinha (1587 to 1522 Ma) and Santa Helena (1485 to 1425 Ma) orogens (Geraldes et al., 2001) and was intruded into the Alto Jauru Group.

The Cachoeirinha orogen consists of the Alvorada (1.53 to 1.44 Ga) and Santa Cruz (1.56 to 1.52 Ga) intrusive suites. These suites are represented by granite, tonalite, granodiorite and gneissic migmatite (Geraldes et al., 2001), and show an Andean-type arc signature with $\varepsilon_{Nd(t)}$ values varying from -1.3 to +2.0 and T_{DM} ages of 1.9 to 1.7 Ga (Bettencourt et al., 2010; Geraldes et al., 2001). The Santa Helena orogen comprises the Santa Helena (1.44 to 1.42 Ga), the Pindaituba (1.46 to 1.42 Ga) and the Água Clara (1.44 to 1.42 Ga) intrusive suites (Ruiz, 2005). The intrusive suites of the Santa Helena Orogen consist of monzonites, granodiorites and tonalites in an oceanic-continental arc setting evidenced by $\varepsilon_{Nd(t)}$ values varying from +1.0 to +4.0 and T_{DM} ages of 1.8 to 1.5 Ga (Geraldes et al., 2001; Ruiz, 2005).

The Figueira Branca Suite is a layered mafic-ultramafic complex composed from bottom to top of dunite, pyroxenite, gabbro-norite, anorthosite, thin layers of troctolite, and olivine-gabbro (Teixeira et al., 2011). The Indiavaí gabbro from the suite yielded a U-Pb SHRIMP zircon age of 1425 ± 8 Ma (Fig. 1b, box I), and a second intrusion near Cachoeirinha city (Fig. 1b, box C) was dated at 1541 ± 23 Ma (Teixeira et al., 2011). Ar-Ar dating of biotites yielded plateau ages of 1275 ± 4 Ma and 1268 ± 4 Ma for the Indiavaí gabbro, which were evaluated as minimum ages for regional cooling. $\varepsilon_{Nd(1.42\ Ga)}$ values vary from +3.0 to +4.7, and $\varepsilon_{Sr(1.42\ Ga)}$ values from -39.1 to -8.1 indicating a predominantly juvenile source (Fig. 2). The crystallization age of the Indiavaí gabbro is coeval with the later stages of evolution of the Santa Helena Orogen (Fig. 1b) (Tassinari et al., 2000).

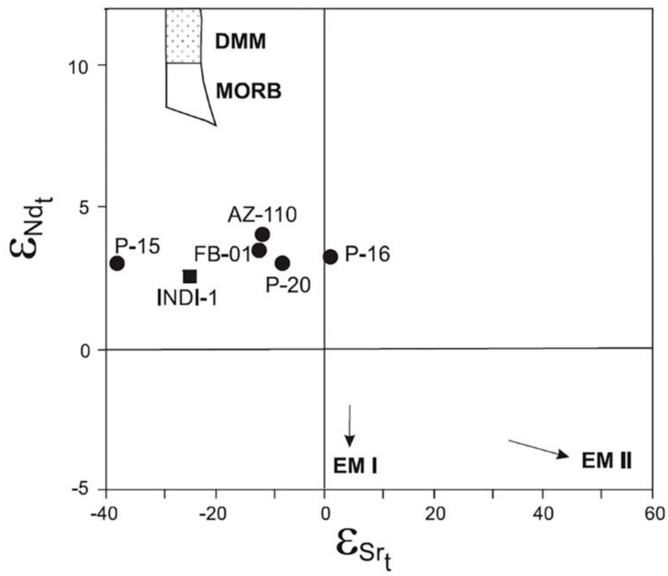

Fig. 2 - ε_{Nd} (1.42 Ma) vs. ε_{Sr}(1.42 Ga) diagram of the Figueira Branca Suite (Teixeira et al., 2011).

Our study is focused on the geological, geophysical, isotope and geochemical character of four northwest aligned intrusions of the Figueira Branca Suite between the towns of Indiavaí and Lucialva (Fig. 3). This data set provided a basis for evaluating other bodies with similar features usually associated with this suite (Fig. 1). By associating different bodies of similar geophysical signature with the Figueira Branca Suite, we were able to estimate the extent of the magmatism that generated the suite during the Mesoproterozoic and its role for the tectonic framework of the area.

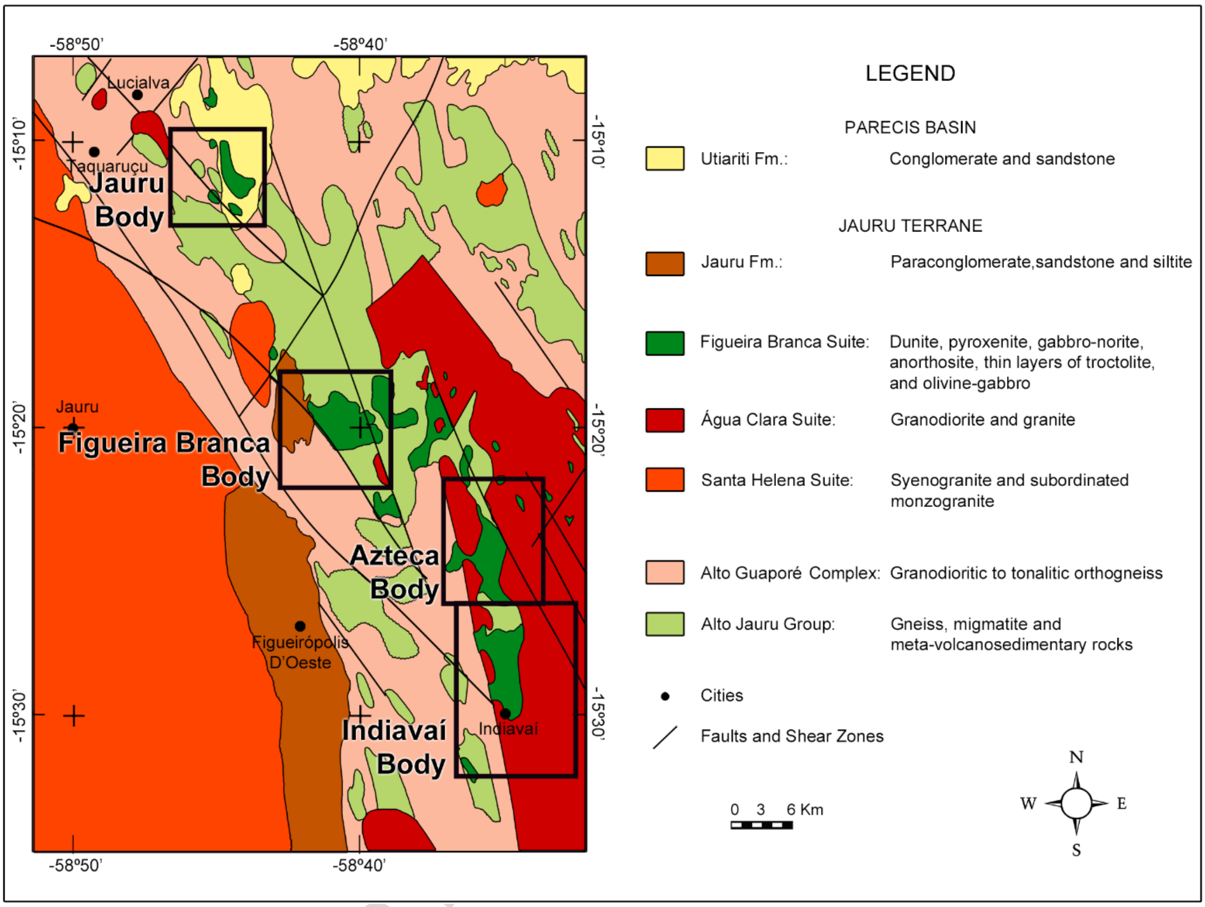

Fig. 3 – Local geological map (Nunes, 2000a; Saes et al., 1984; Teixeira et al., 2011).

Bettencourt et al. (2010) suggested rocks of the Figueira Branca Suite mafic-ultramafic suite extend north of the Santa Helena batholith. In more detailed studies, Ruiz (2005), Corrêa da Costa et al. (2009) and Girardi et al. (2012) associate the mafic-ultramafic plutons to the north of the Santa Helena batholith to the Córrego Dourado Suite (Fig. 1). This suite is made of foliated metagabbro, metatroctolite, tremolite, pyroxenite and serpentinite (Corrêa da Costa et al., 2009; Ruiz, 2005). Although there is no direct dating of the Córrego Dourado

Suite, Ruiz (2005) associate the rock type and deformation of this suite to the 1439 ± 4 Ma Salto do Céu gabbroic sill (Teixeira et al., 2016).

Northwest of the Jauru Terrane, a set of mafic-ultramafic intrusions crops out in the Alto Guaporé Metamorphic Complex. (Nunes, 2000b) associated these bodies, the Morro do Leme and the Morro do Sem-Boné suites, to the Cacoal Suite (not mapped in Fig. 01, more outcrops are found to the north of Fig. 1). These suites are basic-ultrabasic intrusions, made up of dunites and peridotites of 1349 ± 14 Ma (Rb-Sr, whole rock) (Quadros and Rizzotto, 2007).

3. *Data*

In 2006, the Brazilian Geological Service undertook a gamma-ray and magnetic field airborne survey named "Projeto 1080 – Área 2 Mato Grosso" that covers the region occupied by the Figueira Branca Suite. The nominal terrain clearance was 100 m at an airspeed of approximately 280 Km/h. The north-south line spacing was 500 m, whereas the east-west tie lines were spaced at 10000 m. The airborne survey was processed by LASA Prospecções S/A and Prospectors Aerolevantamentos e Sistemas LTDA.

The gamma-ray data were measured with an Exploranium GR-820 Spectrometer of 256 channels. This spectrometer uses 5 sets of NaI (Tl) crystals, three of them downward-oriented, and two upward. The downward-oriented sets are composed by two sets crystal of 16.8 L and one set of 8.4 L. The two upward-oriented sets contain 4.2 L crystals. The sampling interval was 1 s, resulting in an observation spacing of approximately 78 m.

The acquisition of the magnetic field data used Geometrics G-822A Cesium magnetometers of resolution of 0.001 nT. The sampling interval of 0.1 s resulted in an approximate sample spacing of 7.8 m. The magnetic noise level is 0.5 nT after the industry standard corrections were applied. The average International Geomagnetic Reference Field (IGRF) ambient field for this period, which had an inclination -11.6°, declination 234.9°, and intensity 23749 nT.

195 ground gravity stations were installed in the region where the suite is emplaced. 50 samples of different rock types were collected for petrophysical and geochemical measurements. Density data were collected by the "Archimedes method" with distilled water and a high-precision analytic balance, whereas magnetic susceptibility measures were taken using a Kappameter KT-9 magnetic susceptibility meter. Thin sections were prepared and analysed to select samples for geochemical measurements and for constraining the geophysical models. 30 samples were selected for whole-rock major elements analyses through XRF, from which 20 were designed for trace and rare-earth elements analyses by ICP-MS, containing specimens of the Figueira Branca Suite, Alto Jauru Group and adjacent granitic suites.

The selected samples were powdered and homogenized as bulk material. The XRF analyses were made in a Philips PW2400 XRF instrument at the Geoanalítica laboratory of the Instituto de Geociências of the Universidade de São Paulo, Brazil. The trace and REE analyses were made at the Laboratório de Geoquímica Analítica of the Universidade Estadual de Campinas, Brazil. The samples were digested in Parr-type bombs with HF and HNO_3 mix. All solutions were prepared with ultra-pure water through the Milli-Q system. The HNO_3 was purified by sub-ebulition. The containers used on the dilutions were previously cleaned with HNO_3 (5%) and washed with ultra-pure water. The trace elements measurements used an ICP-MS XseriesII (Thermo) equipped with CCT (Collision Cell Technology). The calibration of the equipment was made using multielementary solutions gravity-prepared by monoelementary standard solutions of 100 mg/L (AccuStandards). The detection limit ($DL = x + 3\sigma$) was determined as the average (x) plus three standard deviations (σ) of ten measurements of the laboratory blanks and the instrument background. The quality control used the reference materials BRP-1 (basalt) and GS-N (granite) from the Laboratório de Geoquímica Analítica. The results and their respective uncertainties for the eleven samples from the Figueira Branca Suite rocks are available in Table 1.

Table 1 – XRF and ICP-MS results for the Figueira Branca Suite.

XRF Results (%)													
Sample	IND03	IND06	IND09	IND10	AZT05	AZT10	FIG01	FIG02	FIG03	JAU01	JAU02	DL	Error (±)
SiO2	47.09	46.96	47.79	47.04	50.97	48.39	48.89	39.64	40.74	49.48	50.18	0.03	0.48
TiO2	0.41	0.35	0.26	0.28	0.57	0.42	0.22	0.06	0.08	0.28	0.55	0.003	0.009
Al2O3	20.48	23.95	21.72	20.7	18.37	18.1	6.15	9.39	18.13	21.18	17.62	0.02	0.09
Fe2O3	9.89	6.52	8.04	9.08	8.25	8.45	9.31	11.3	6.64	7.7	9.36	0.01	0.09
MnO	0.14	0.09	0.11	0.12	0.14	0.13	0.17	0.15	0.09	0.1	0.14	0.002	0.003
MgO	9.01	7.09	8.79	9.83	7.27	5.67	22.96	26.97	16.26	7.66	10.56	0.01	0.06
CaO	10.27	12.35	11.02	10.3	9.43	10.5	7.89	4.92	9.4	10.02	8.73	0.01	0.02
Na2O	2.38	2.13	2.46	2.36	2.75	2.22	0.32	0.33	1.13	2.76	2.37	0.02	0.12
K2O	0.12	0.11	0.11	0.12	0.38	0.81	0.21	0.03	0.03	0.19	0.24	0.01	0.01
P2O5	0.03	0.03	0.01	0.02	0.04	0.02	0.12	0.01	0.01	0.01	0.11	0.003	0.003
LOI	<0.01	0.86	0.1	0.16	1.48	5.72	5.28	7.98	6.98	0.16	0.2	0.01	---
Total	99.81	100.44	100.41	100.02	99.65	100.43	101.52	100.78	99.49	99.54	100.06	---	---
ICP-MS Results ($mg.g^{-1}$)													
Sample	IND03	IND06	IND09	IND10	AZT05	AZT10	FIG01	FIG02	FIG03	JAU01	JAU02	DL	Error (±)
Cu	89.1	---	32.5	---	74.3	35.3	4.89	32.0	12.9	46.6	42.6	3	0.2
Nb	0.52	---	0.37	---	1.53	0.75	0.61	0.32	1.33	0.20	1.38	0.9	0.05
Rb	4.31	---	3.58	---	11.4	13.8	0.93	0.94	0.81	3.55	3.41	1	0.2
Sr	238	---	236	---	218	218	178	137	225	522	458	6	0.07
Zn	55.9	---	46.1	---	59.2	45.9	58.7	63.1	41.4	52.3	71.5	2	3.4
Zr	17.4	---	13.4	---	42.8	22.6	13.0	3.30	5.13	4.74	32.9	5	0.04
Cr	17.2	---	32.5	---	390	103	1703	136	1184	137	609	1	0.4
Ba	41.7	---	39.0	---	85.5	71.6	8.47	24.9	28.0	112	154	7	0.08
Ni	202	---	160	---	40.7	49.6	1054	1112	720	168	175	0.9	0.2
Be	0.15	---	0.09	---	0.35	0.23	0.39	0.06	0.04	0.16	0.32	0.1	0.04
V	100	---	65.6	---	139	134	110	19.8	26.9	69.7	112	7	0.1
Co	56.8	---	52.9	---	40.3	39.3	82.9	125	70.7	50.7	54.1	1.4	0.02
Ga	16.3	---	15.9	---	19.0	17.1	5.65	5.99	10.6	16.3	15.3	0.6	0.009
Y	8.87	---	6.19	---	14.7	10.6	5.43	1.56	1.77	3.12	8.85	1	0.02
Mo	0.10	---	0.08	---	0.28	0.14	0.13	0.08	0.08	0.06	0.15	0.1	0.02
Sn	0.14	---	0.06	---	0.32	0.19	0.06	<DL	<DL	<DL	0.14	0.4	0.08
Sb	0.03	---	0.02	---	0.14	0.10	0.39	0.01	0.01	0.01	0.01	0.01	0.01
Cs	0.06	---	0.05	---	0.83	0.40	0.02	0.14	0.15	0.11	0.19	0.02	0.004
Hf	0.53	---	0.42	---	1.20	0.69	0.35	0.09	0.13	0.16	0.81	0.2	0.005
Ta	0.05	---	0.09	---	0.12	0.05	0.05	0.09	0.40	0.03	0.08	0.08	0.003
Pb	0.57	---	0.51	---	1.78	1.47	1.09	0.28	0.25	0.67	1.04	0.3	0.05
Bi	0.03	---	0.03	---	0.04	0.08	0.06	0.02	0.02	0.02	0.02		0.006
Th	0.28	---	0.22	---	0.85	0.33	0.46	0.14	0.05	0.05	0.14	0.1	0.003
U	0.08	---	0.05	---	0.39	0.12	0.33	0.19	0.06	0.01	0.08	0.03	0.03
La	1.82	---	1.47	---	5.31	2.70	4.02	0.96	0.90	1.57	5.08	1	0.01
Ce	4.13	---	3.28	---	11.5	6.16	8.37	1.75	1.99	3.02	11.7	1.2	0.02
Pr	0.60	---	0.46	---	1.51	0.87	1.15	0.24	0.27	0.37	1.60	0.2	0.006
Nd	2.95	---	2.20	---	6.77	3.97	4.85	0.93	1.10	1.66	6.98	0.9	0.009
Sm	0.98	---	0.69	---	1.78	1.17	1.08	0.21	0.27	0.45	1.61	0.2	0.007
Eu	0.49	---	0.46	---	0.63	0.60	0.28	0.14	0.19	0.47	0.71	0.08	0.003
Gd	1.13	---	0.80	---	1.96	1.36	1.03	0.21	0.27	0.44	1.57	0.3	0.006

Tb	0.22	---	0.16	---	0.36	0.26	0.16	0.03	0.05	0.07	0.26	0.05	0.003
Dy	1.57	---	1.10	---	2.56	1.88	0.98	0.26	0.31	0.53	1.61	0.3	0.003
Ho	0.36	---	0.24	---	0.54	0.40	0.20	0.05	0.07	0.11	0.34	0.06	0.003
Er	0.96	---	0.67	---	1.56	1.17	0.53	0.14	0.18	0.31	0.94	0.1	0.004
Tm	0.14	---	0.10	---	0.22	0.17	0.08	0.02	0.03	0.05	0.13	0.02	0.02
Yb	0.91	---	0.60	---	1.44	1.05	0.51	0.17	0.18	0.34	0.86	0.09	0.005
Lu	0.14	---	0.10	---	0.22	0.17	0.08	0.03	0.03	0.05	0.14	0.02	0.002
Sc	14.7	---	13.5	---	27.2	29.2	21.3	5.95	4.74	12.2	20.3	0.8	1.4
Li	4.20	---	7.44	---	8.97	5.31	1.39	3.72	2.68	5.68	5.76	0.3	0.03
Cd	0.07	---	0.05	---	0.09	0.07	0.05	0.01	0.01	0.07	0.07	0.1	0.02

4. Results & Discussion

4.1. Typical Magnetic Field Signature and Bodies Associated with the Suite

Initial data analysis used magnetic field method and the gamma-ray spectrometry to establish the geophysical signature of the Figueira Branca Suite and delineate analogue anomalies within the Jauru Terrane. The "Projeto 1080 – Área 2 Mato Grosso" provided a regional data set of magnetization contrasts and gamma-ray emissions (Fig. 4). The four recognized bodies of the Figueira Branca Suite display significant contrasts of magnetization with their respective host-rocks, generating magnetic anomalies in the total magnetic field map (Fig. 4a). The intrusions were named, from the south to north, Indiavaí, Azteca, Figueira Branca and Jauru. These anomalies show a specific pattern with negative values to the north and positive to the south, indicating the presence of a significant remanent magnetization in their sources. The gamma-ray emission for the areas of the four bodies indicated discrete low counts (dark to black areas in Fig. 4b), typically associated with mafic rocks (Dickson and Scott, 1997). The Indiavaí and Azteca bodies show the general low counts pattern, but have higher concentrations of eTh and eU than their northern counterparts. The higher concentration of both elements produces a cyan coloration in the area of the bodies.

A group of small occurrences associated to the Figueira Branca Suite is found to the east of the Figueira Branca anomaly and to the north of Azteca (Fig. 4a). This anomaly shows a low trend of gamma-ray counts (Fig. 4b) as expected for mafic rocks, however the magnetic signature differs grandly from the other anomalies linked with the suite.

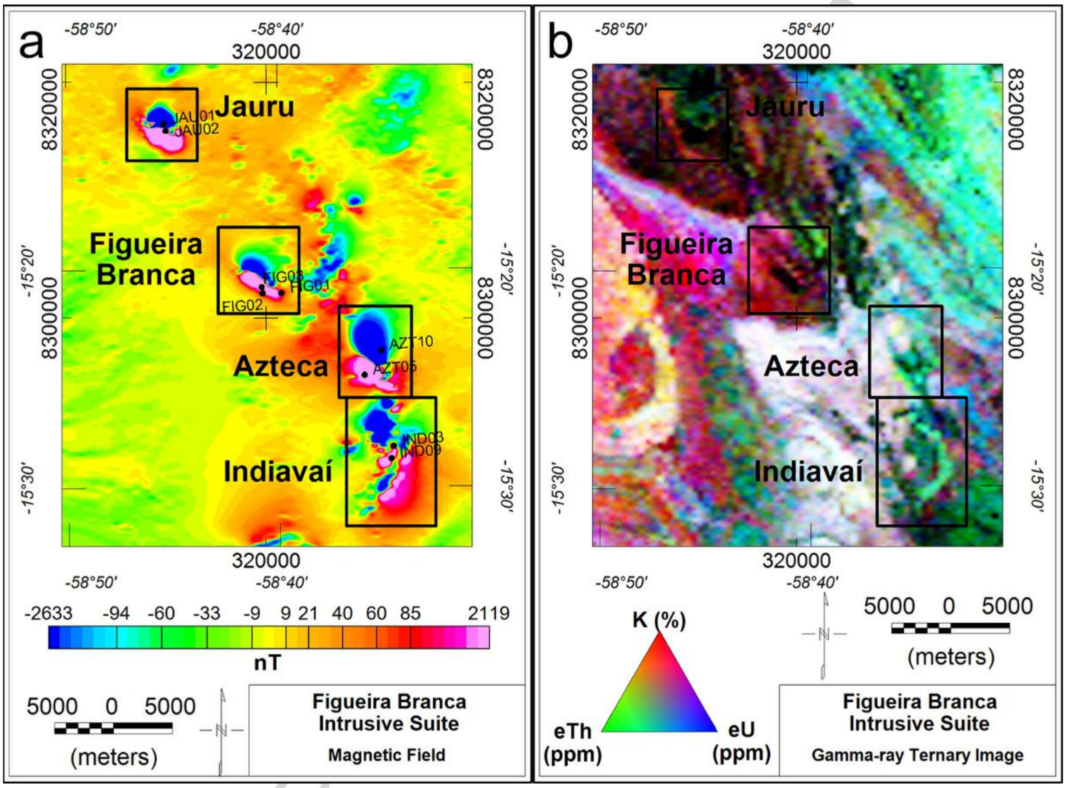

Fig. 4 - (a) Total field anomalies of the area of the Figueira Branca Suite, including the location of the samples associated to the intrusive suite. (b) Gamma-ray emission of the area.

The magnetic field and gamma-ray emissions were used as proxies to investigate for additional mapped and unmapped intrusions related with the Figueira Branca Suite. To use the magnetic field as a proxy, we applied the Reduction to the Magnetic Pole (RTP) operator to estimate the inclination and declination of the total field anomalies. A successful RTP filtering results in a magnetic field where the anomalies present positive contrasts centred over the limits of the bodies, as the negative values on the map are close to zero. The RTP filtering requires knowledge of the direction of total magnetization of the field. Hence, it is recommended to use of this filtering in areas with magnetic anomalies predominantly generated by the induced magnetization, where its direction is known by the geomagnetic field in the area during the survey. Fedi et al. (1994) and Cordani and Shukowsky (2009) proposed and implemented, respectively, a technique called MaxiMin, which does an inversion of the inclination and declination to estimate the values that better minimize the negative values of the field and maximize the positive values. The MaxiMin optimal results were inclination of 56º and declination of 213º, with an α_{95}º of 5º after 386 iterations. Figure 5a shows the RTP field of the Jauru Terrane with the targets found with the analogue characteristics of gamma-ray emission and/or magnetization. In order to define the lateral limits of the bodies and evaluate qualitatively the MaxiMin results, we used the 3-D Amplitude of the Analytic Signal (Fig. 5b and d) (Roest et al., 1992).

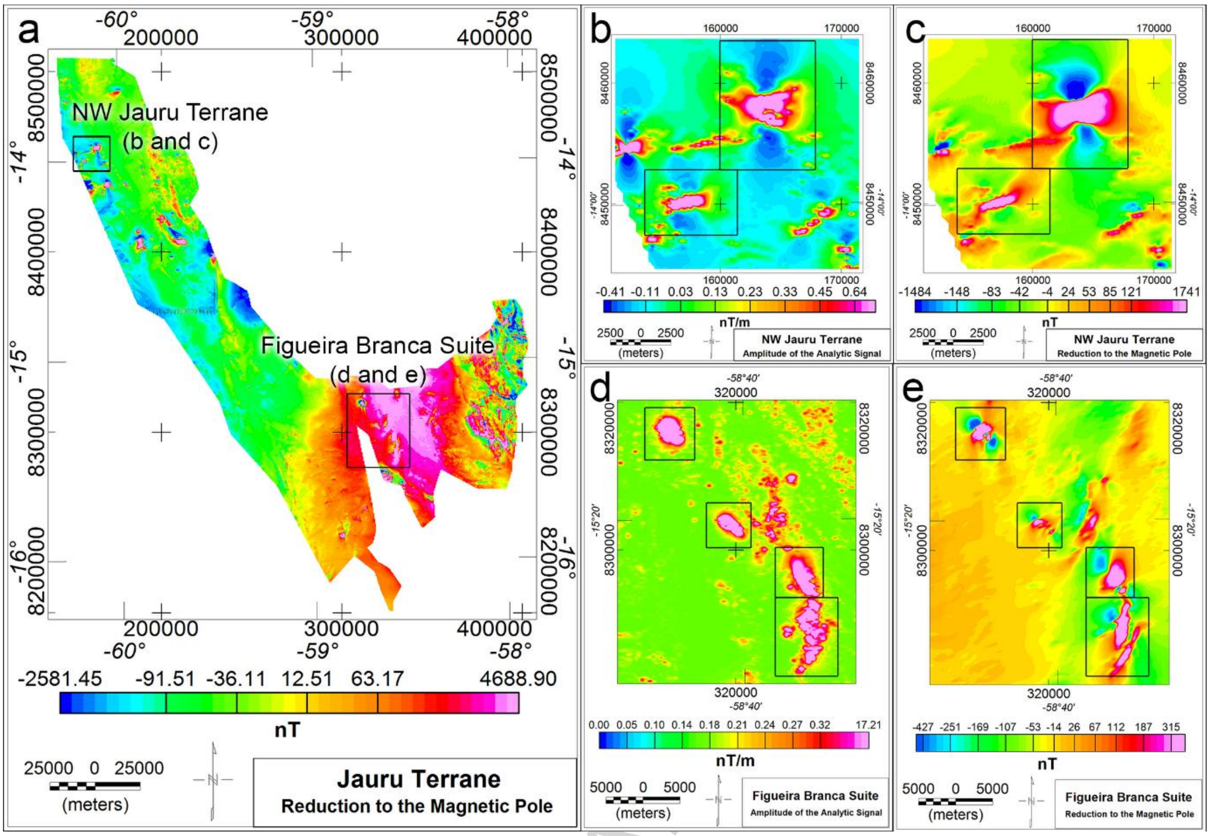

Fig. 5 – (a) RTP of the Jauru Terrane identifying bodies with similar features as those already recognized as part of the Figueira Branca Suite. (b) and (c) are the Amplitude of the Analytic Signal and the RTP, respectively, of the anomalies in the northwest of the Jauru Terrane, while (d) and (e) are the same maps, respectively, for the Figueira Branca Suite.

In the northwest of the Jauru Terrane, a set of other gamma-ray and/or magnetic anomalies presented similar geophysical signature inside the Jauru Terrane. The only two anomalies in the northwest that were properly reduced to the pole were spatially associated with the Morro do Leme and the Morro do Sem-Boné complexes (Fig. 1, 5b and c). These intrusive complexes are associated to Cacoal basic-ultrabasic intrusive suite and hosted by the Alto Guaporé Belt (Nunes, 2000b). The RTP of both complexes present similar shapes, indicating analogue direction of total magnetization. Louro et al. (2014) suggest a remanent magnetization with inclination of 41.8º and declination of 193º for the Morro do Leme. Therefore, in the absence of analogue geophysical signatures unrelated with known suites in the Jauru Terrane, we focused on characterizing the Figueira Branca Suite using the only the four recognized bodies that maintained the same signature on different and independent geological and geophysical data.

4.2. Gravity Field

The gravity field of the region showed three of the four gravity anomalies (Fig. 6). The Figueira Branca anomaly could not be properly surveyed due to flooding over the northern part of the body due to construction of a dam. The irregular distribution of gravity stations allied with a regional trend of the gravity field requiring regional-residual separation. We isolated the gravity anomaly signatures using a high-pass filter to remove wavelengths larger than 24400 Km. The cut-off wavelength was defined based on the first inclination change of the energy spectrum. The anomalies showed good spatial correlation with the magnetic field data and their maximum amplitudes varied from 1.6 (in the Figueira Branca magnetic anomaly area) to 7.6 mGal.

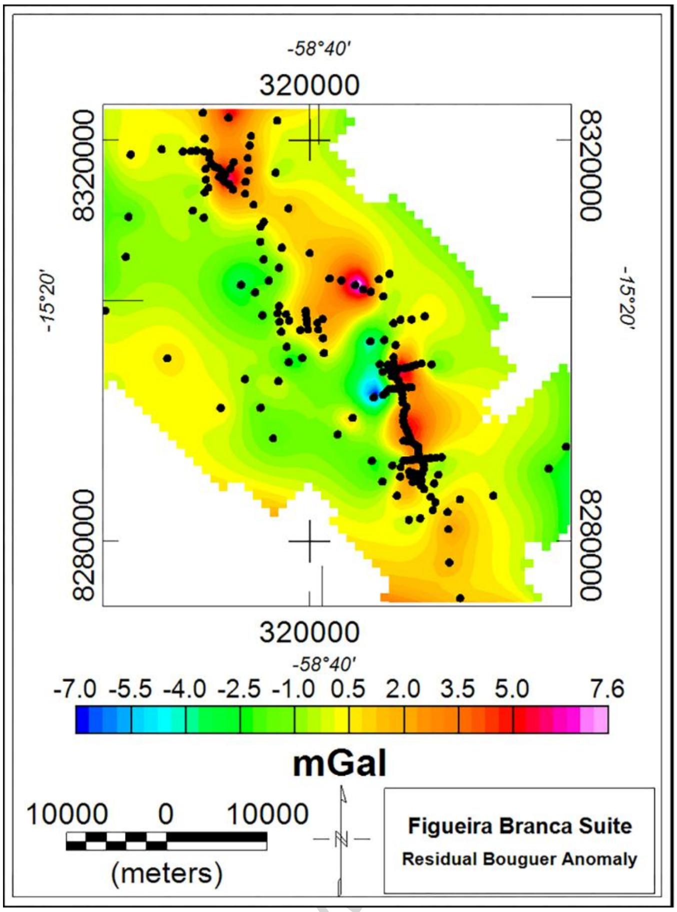

Fig. 6 – Residual Bouguer anomaly map of the Figueira Branca Suite. The black circles represent the location of the gravity stations.

4.3. *Mineralogy and Geochemical Signature*

Mineralogy of the Indiavaí, Azteca and Jauru bodies is dominated by plagioclase (ca. 60% to 70%) with fractured and serpentinized olivine (ca. 20% to 25%) and intergrown pyroxene (ca. 10% to 15%) (Fig. 7a, 7b and 7c). The Figueira Branca intrusion shows variable grain size with parts relatively fined grained and displaying significant serpentinization and weathering (Fig. 7d), whereas other sections are coarse grained and contain a higher proportion of olivine (ca. 60% olivine and ca. 40% plagioclase; Fig 7e and 7f). Opaque oxide minerals are present in all thin sections. D'Agrella-Filho et al. (2012) determined the opaque oxide phase as magnetite in the Indiavaí gabbro.

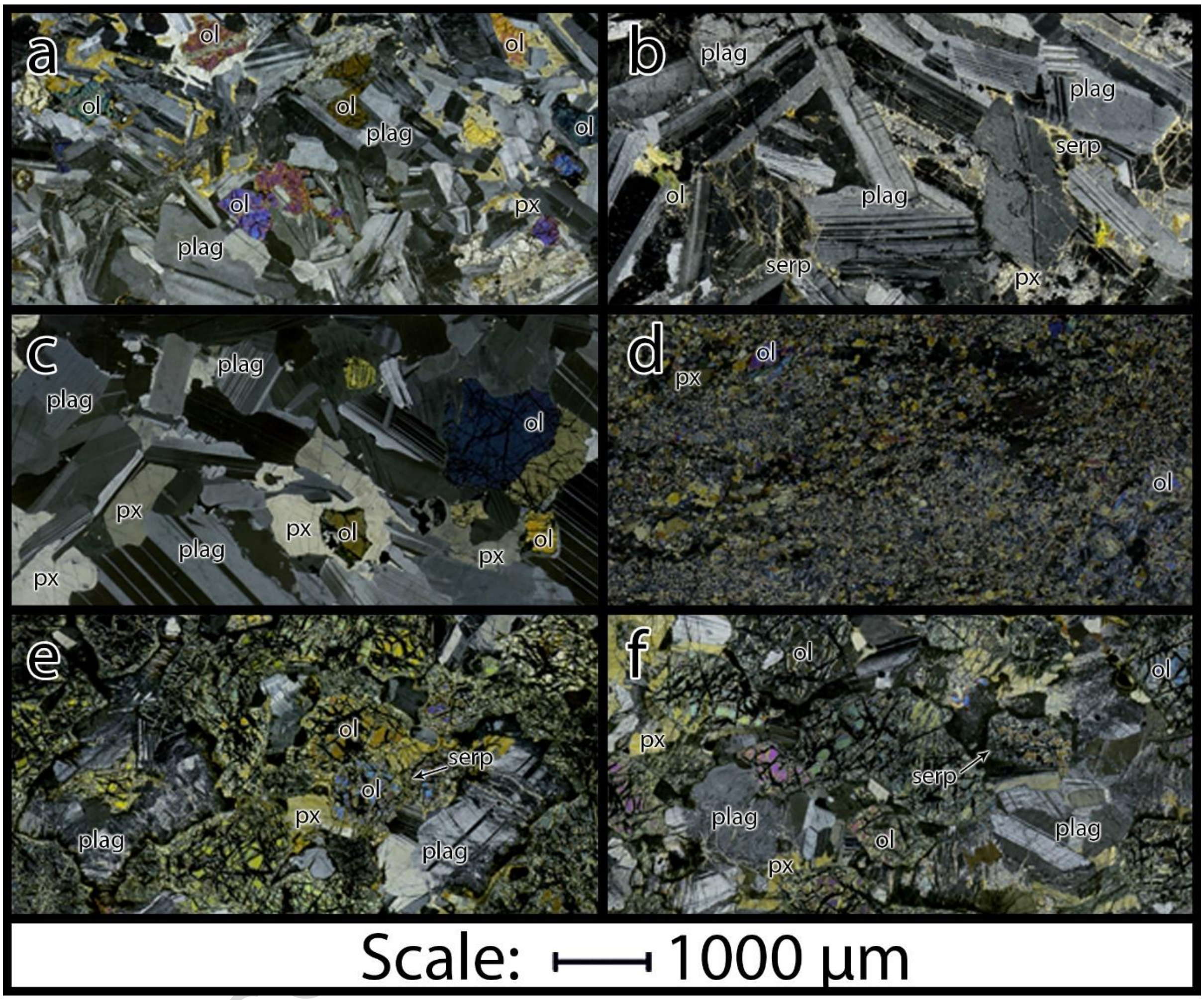

Fig. 7 – Thin sections of the samples (a) IND09, (b) AZT05, (c) JAU01, (d) FIG01, (e) FIG02 and (f) FIG03. The crystals are indicated by their abbreviations: ol – olivine, plag – plagioclase, px – pyroxene, and serp – serpentine. All photos were taken with cross-polarized light.

Geochemical data were collected on 11 samples (Table 1). On a TAS (SiO_2 vs. $NaO_2 + K_2O$) plot (Fig. 8a) (Middlemost, 1994), these samples were located inside the gabbro field, with the exception of two out of three olivine-rich samples from the Figueira Branca intrusion (FIG01 and FIG02) that showed significantly lower values of SiO_2 and Na_2O+K_2O and were located in the peridotite-gabbro field (Fig. 8a).

The REE normalized to chondrites (Mcdonough and Sun, 1995) shows the increase in the slopes among the intrusions, from lower to higher: Indiavaí, Figueira Branca, Azteca and Jauru (Fig. 8b). The increase in the slopes indicate the evolution of the magma of the Figueira Branca Suite, with the Jauru body representing the most, and the Indiavaí intrusion the least, evolved. The majority of the samples display Eu anomalies consistent with the presence of plagioclase (Fig. 7).

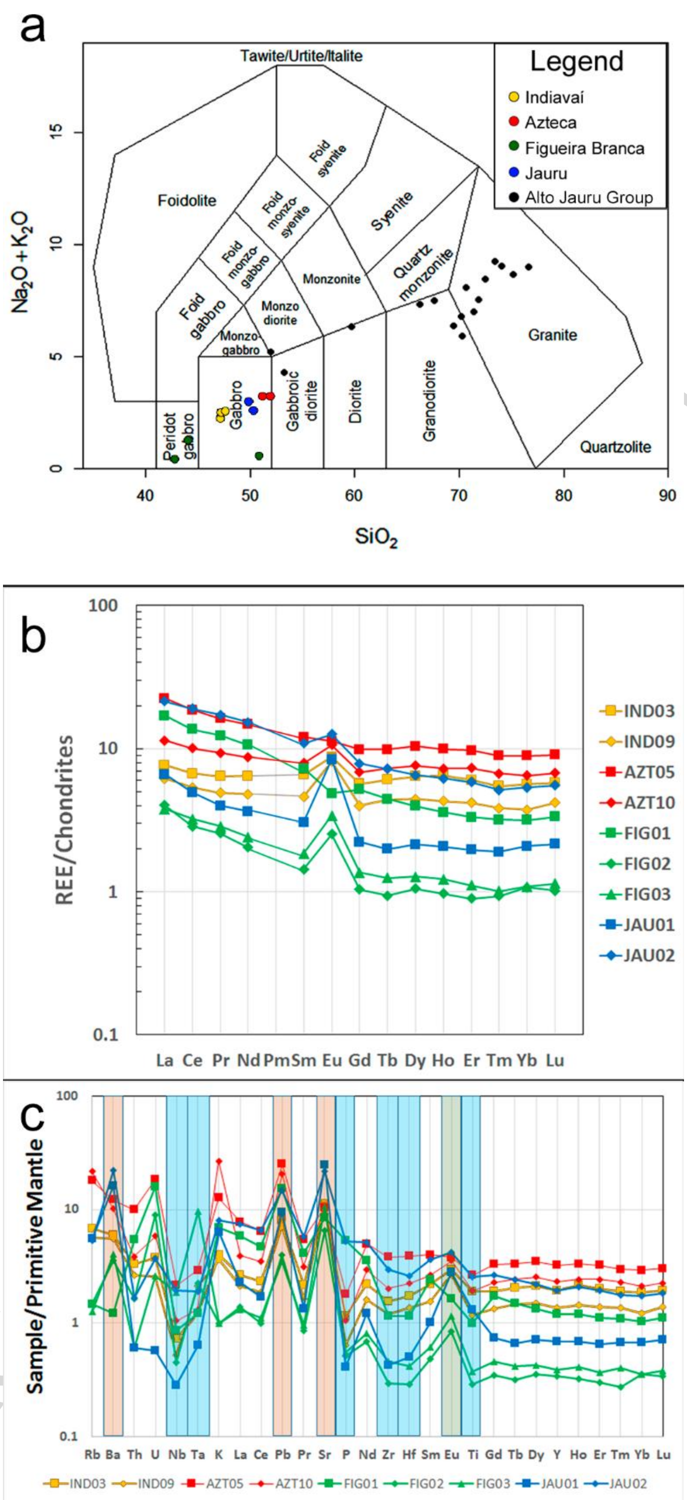

Fig. 8 – (a) TAS (SiO2 vs. NaO2 + K2O) plot (Middlemost, 1994), (b) REE normalized to the chondrite values (Mcdonough and Sun, 1995) and trace elements normalized to Primitive Mantle (Sun and McDonough, 1989) of the Figueira Branca Suite.

According with Zheng (2012), Pb and Sr positive anomalies on a Primitive Mantle normalized spidergram (Sun and McDonough, 1989) are associated to metasomatism in subduction zones before the melting of the parental magma (Fig 8c). Two types of metasomatized media are possible in these zones: a media characterized by slab-derived fluids and one by hydrous melt. The first has high capacity to transport water-soluble elements, but not water-insoluble. Hydrous melts, however, can transport both water-soluble and insoluble elements. Rb/Y, Nb/Y, Nb/Zr and Th/Zr ratios can be used as proxies to suggest the type of metasomatized media (Kepezhinskas et al., 1997). The mafic samples of the Figueira Branca Suite indicated high values of Rb/Y and Th/Zr, and lower values of Nb/Y and Nb/Zr (Fig. 9a and 9b), indicating a hydrous melt predominance in the parental magma. The samples of the Figueira Branca intrusion showed significantly different Th/Zr and Nb/Zr ratios than the remaining samples from the suite. This behaviour follows the contrast observed on the mineralogy (Fig. 7c) and REE slopes (Fig. 8b) of these samples.

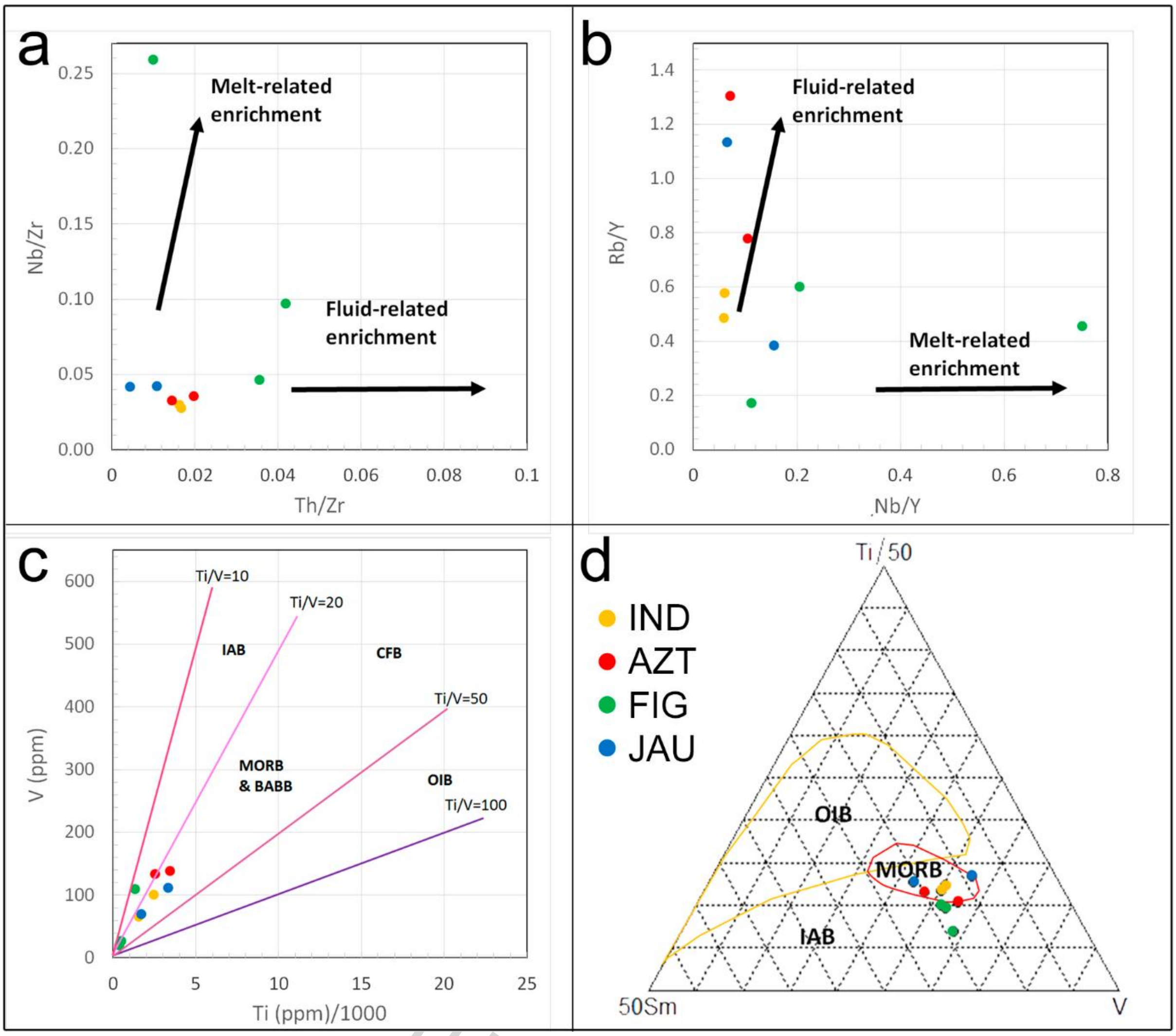

Fig. 9 – Petrogenetic diagrams (a) Nb/Zr vs. Th/Zr, and (b) Rb/Y vs. Nb/Y (Kepezhinskas et al., 1997), and tectonic discriminant (c) V vs. Ti/1000 (Shervais, 1982), and (d) ternary Ti/50 vs. Sm*50 vs. V (Vermeesch, 2006) of the Figueira Branca Suite.

Pronounced Zr and Hf negative anomalies for the Figueira Branca Suite samples (Fig. 8c) is indicative of a supra-subduction setting (Wang et al., 2013) and consistent with the Rb/Y, Nb/Y, Nb/Zr and Th/Zr ratios (Fig. 9a and b). The samples show Ti/V ratios (10>Ti/V>30) (Fig. 9c) related with MORB and Back-Arc Basin Basalts (BABB) (Shervais, 1982), whereas in the ternary Ti-Sm-V diagram (Vermeesch, 2006) (Fig. 9d), they fall in the transitional field between MORB and IAB. Vermeesch (2006) explains that the multiplying factors in the Ti-V and Ti-Sm-V diagrams are used because geochemical data is expressed as parts of a whole, so the concentration of some elements are not entirely independent to vary without interfering in the concentration of others in the same system.

The Figueira Branca Suite lies to the east of the Santa Helena orogen and to the west of the Água Clara orogen (Fig. 1), two structures originated by the subduction of oceanic crust to the west of the Santa Helena orogen. These features, along with the ε_{Nd}(1.42 Ma) vs. ε_{Sr}(1.42 Ga) signature (Fig. 3), suggest that the Figueira Branca parental magma, originally depleted, metasomatized during and/or after the subduction of the same ocean crust that resulted in the Santa Helena and Água Clara orogens. Furthermore, the location of the suite between orogens and the parallel alignment of the geophysical anomalies with the extinct subduction zone, in an extensive environment (Teixeira et al., 2011), suggests a tectonic framework of back-arc magmatism.

4.4. Magnetic and Gravity Modelling

Density and magnetic susceptibility were measured on samples of the Figueira Branca Suite and adjacent rocks (Table 2). These values, along with the total field direction estimated by the MaxiMin technique (inclination 56º and declination of 213º), were used as constraints to develop magnetic and gravity models for the four anomalies of the Figueira Branca Suite. We adapted the methodology of staged inversion of Foss (2006) for the available dataset. First, we created outcropping block models with lateral limits based on the amplitude of the analytic signal over the magnetic field data. To each of these models were attributed the total magnetization direction, the average magnetic susceptibility and density (Table 2). The ambient magnetic field was defined by the IGRF by the time of the survey (inclination -11.6°, declination 234.9°, and intensity 23749 nT). The significantly smaller number and mostly irregularly distributed gravity data, was modelled as a secondary parameter which we allowed larger root mean square (RMS) errors (less than 20%) than to the magnetic field (less than 10%).

Table 2 - Measured average density and magnetic susceptibility of the four bodies of the Figueira Branca Suite.

Body	Average Density (g/cm^3)	Average Magnetic Susceptibility (SI)
Indiavaí	2.93888 ± 0.0001	0.043 ± 0.003
Azteca	2.91945 ± 0.0001	0.065 ± 0.004
Figueira Branca	2.84133 ± 0.0001	0.054 ± 0.004
Jauru	3.02962 ± 0.0001	0.066 ± 0.005

The staged inversion varied the following parameters at each stage: (1) the amplitude of the total magnetization, and depth extent of the block model; (2) the amplitude of the total magnetization, depth extent and horizontal position; (3) the amplitude of the total magnetization, depth extent, horizontal position and vertices movements in north-south direction; (4) the parameters of the previous stage plus the vertices movements in east-west direction; and (5) all the previous parameters plus the magnetic susceptibility. By the end of the first staged inversion, the body was subdivided in 500 m north-south oriented polygonal prisms centred over the surveyed flight lines and the process was reinitiated to optimize the results, with two differences: instead varying the depth extent in all stages, the vertices were allowed to vary their positions on vertical direction, and the stage (4) was skipped. The third and last pass of inversion permitted the variation of the density of the models, with the modelling based on profiles of the Bouguer anomalies of the Figueira Branca Suite bodies (Figs. 10 and 11).

The models achieved low RMS errors both for the magnetic and gravity data (Table 2). The maps comparing the observed, modelled and residual fields are shown in Figure 10. The modelled Azteca magnetic anomaly (Fig. 10b) showed higher amplitudes in the south of the map unrelated to any model. We attributed the higher amplitude to border effects due to interpolation of the modelled data. The observed Bouguer anomaly profiles are compared with the modelled profiles in figure 11. The residual fields presented low amplitudes when compared with the amplitude of the anomalies in the observed fields (see the RMS in Table 3). Although the average magnetic susceptibility and average density were used as constraints for the modelling, we allowed their variation during the last stages of the inversion due the small number of fresh samples available. The measured and the modelled values remained the same after the inversion (Tables 2 and 3). The modelled amplitude of the total magnetization varied from 2.8 to 8.6 A/m². These amplitudes, attributed to their respective directions obtained through the MaxiMin RTP, enabled the determination of the total magnetization vectors for the sources of the anomalies. The measured and modelled magnetic susceptibilities, with the characteristics of the ambient field given by the IGRF, permitted the estimation of the induced magnetization vectors on the Figueira Branca Suite modelled bodies. Subtracting the total by the induced magnetization vector of each model, we estimated their remanent magnetization vectors. The calculated remanent magnetization for the four anomalies were quite similar as seen in Table 2. Their directions approximate the average remanent magnetization direction of the Indiavaí gabbro reported by D'Agrella-Filho et al. (2012) with inclination 50.7º, declination 209.8º, and α_{95}º 8.0.

Table 3 - Features and RMS values of the models of the Figueira Branca Suite.

Geophysical Models			
Alto Jauru Group (Host-rock)			
Samples			
Avg. Mag. Suscep.	0.007 (SI)	**# of Samples**	36
Avg. Density	2.70 g/cm³		
Indiavaí			
Samples			
Avg. Mag. Suscep.	0.05 (SI)	**# of Samples**	6
Avg. Density	2.94 g/cm³		
Magnetic and Gravity Fields Inversions			
Magnetization	**Induced**	**Total**	**Remanent**
Inclination (º)	-11.6	56	49.6
Declination (º)	346.9	213	199.5
Intensity (A/m)	0.9	3.8	4.4
RMS-Mag (%)	5.8	**# of Points**	29003
RMS-Grav (%)	18.9	**# of Points**	89
Azteca			
Samples			
Avg. Mag. Suscep.	0.07 (SI)	**# of Samples:**	2
Avg. Density	2.91 g/cm³		
Magnetic and Gravity Fields Inversions			
Magnetization	**Induced**	**Total**	**Remanent**
Inclination (º)	-11.6	56	51.2
Declination (º)	346.9	213	191.8
Intensity (A/m)	1.3	8.6	9.5
RMS-Mag (%)	6.4	**# of Points**	9251
RMS-Grav (%)	12.1	**# of Points**	37
Figueira Branca			
Samples			
Avg. Mag. Suscep.	0.06 (SI)	**# of Samples:**	3
Avg. Density	2.84 g/cm³		
Magnetic and Gravity Fields Inversions			
Magnetization	**Induced**	**Total**	**Remanent**
Inclination (º)	-11.6	56	45.9
Declination (º)	346.9	213	194
Intensity (A/m)	1.1	2.8	3.6
RMS-Mag (%)	3.7	**# of Points**	19206
RMS-Grav (%)	10.8	**# of Points**	17
Jauru			
Samples			
Avg. Mag. Suscep.	0.07 (SI)	**# of Samples:**	3
Avg. Density	3.02 g/cm³		
Magnetic and Gravity Fields Inversions			
Magnetization	**Induced**	**Total**	**Remanent**
Inclination (º)	-11.6	56	51.6
Declination (º)	346.9	213	202.9
Intensity (A/m)	1.3	7.8	8.6
RMS-Mag (%)	3.3	**# of Points**	9893
RMS-Grav (%)	13.8	**# of Points**	28

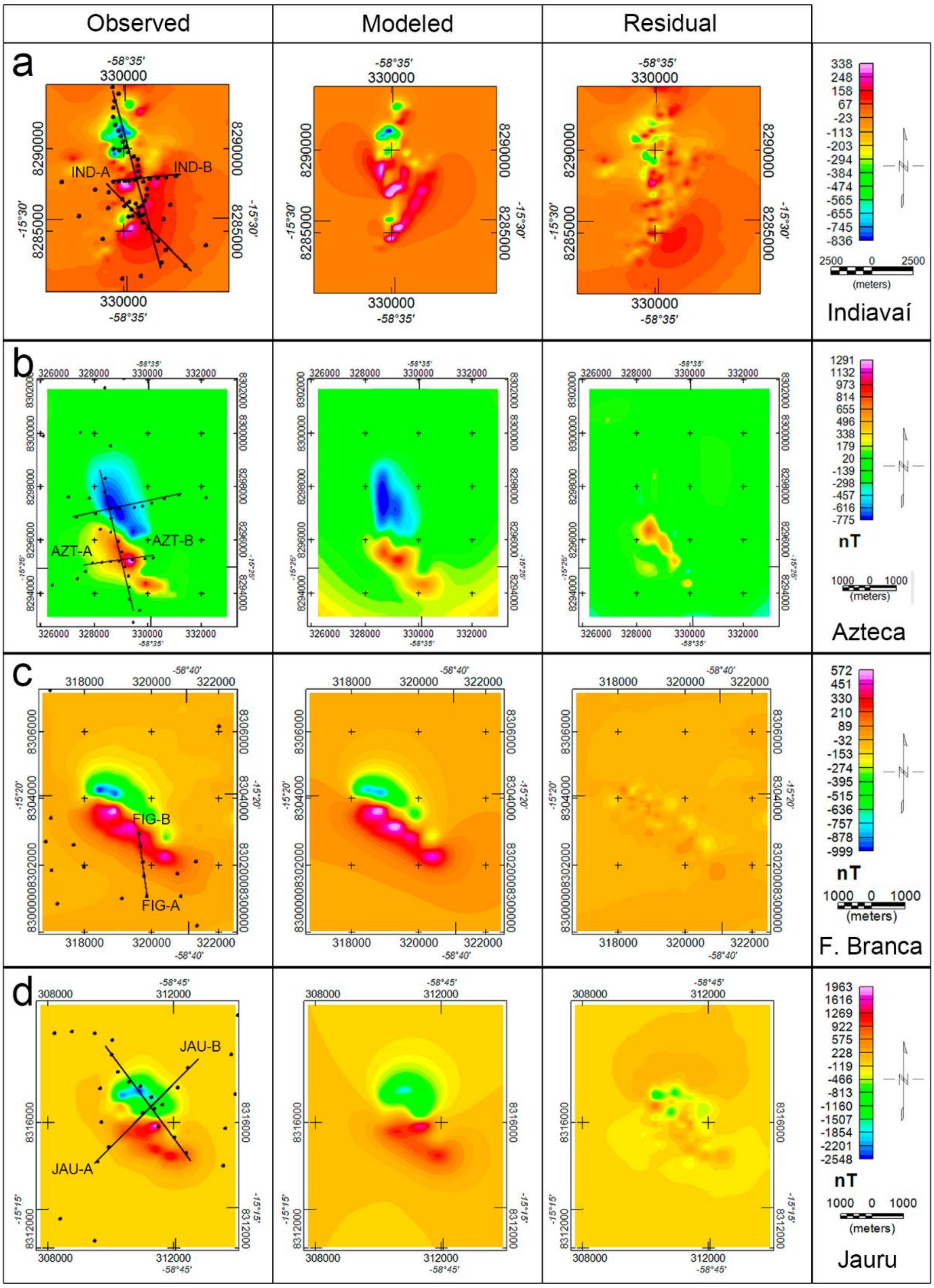

Fig. 10 – Original, modelled and residual magnetic fields of the bodies of Figueira Branca Suite: (a) Indiavaí, (b) Azteca, (c) Figueira Branca, and (d) Jauru. The black circles refer to the gravity measurements. The lines indicate the profiles used in the gravity inversion.

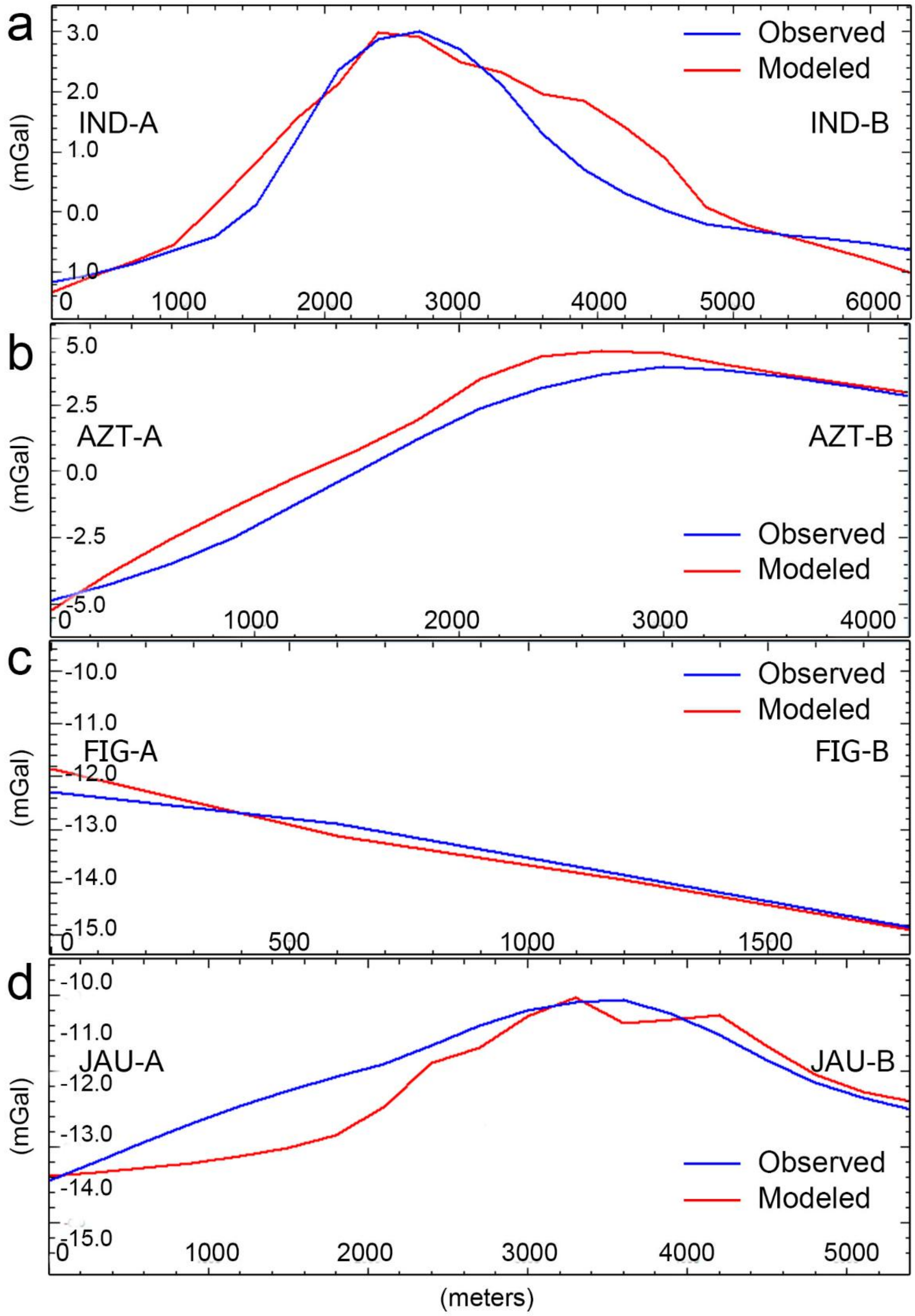

Fig. 11 – Original (blue lines) and modelled (red lines) of the Bouguer anomaly profiles: (a) IND-A to IND-B of the Indiavaí body, (b) AZT-A to AZT-B of the Azteca body, (c) FIG-A to FIG-B of the Figueira Branca body, and (d) JAU-A to JAU-B of the Jauru body.

The modelled bodies display an overall northwest-southeast trend, varying from 6 to 10 km in this direction, whereas their sizes in the northeast-southwest direction varied from 3 to 5 km (Fig. 12). The shallower horizons of the bodies were kept in the surface, constrained by the location the outcrops found in the field, and the vertical extensions ranged from approximately 330 to 835 m. The vertical extension and, by consequence, the depth of the bottom of the bodies are mostly speculative, as the ambiguity inherent to potential field methods does not allow a precise estimation of these features, even considering the knowledge about the magnetic susceptibility, remanent magnetization, and the location of outcrops.

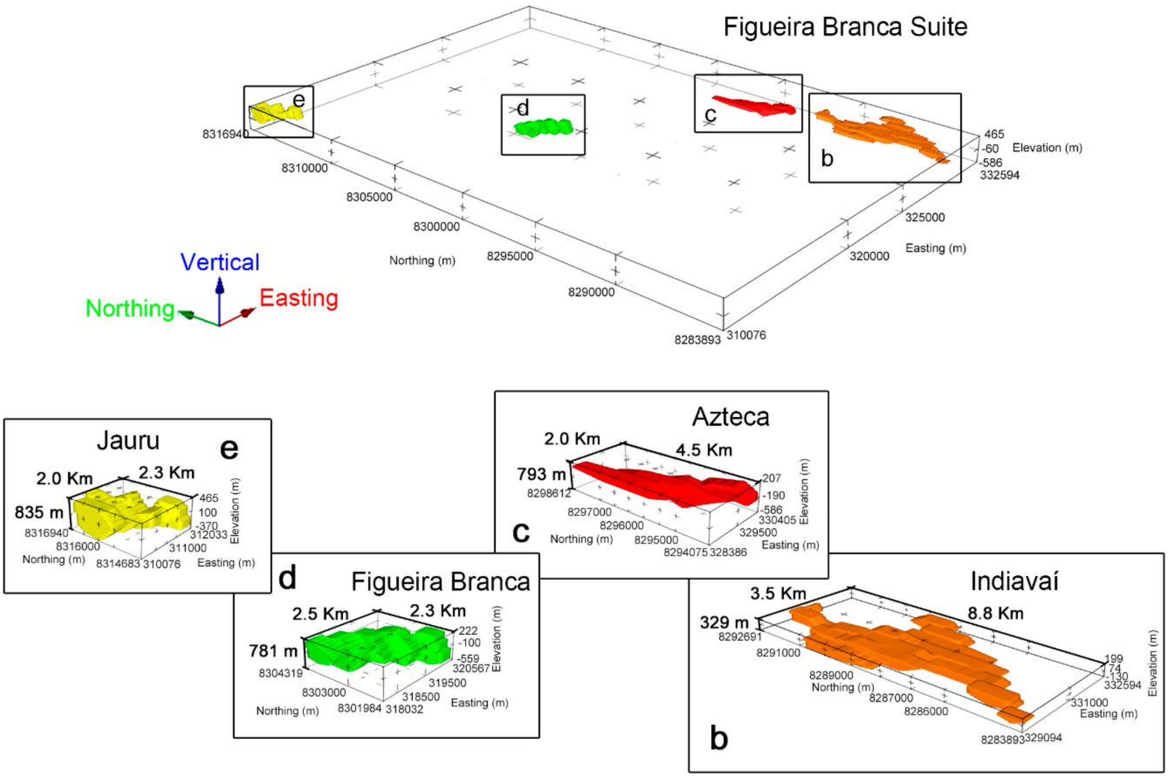

Fig. 12 – Joint magnetic and gravity models of the Figueira Branca Suite. In detail, (a) Indiavaí, (b) Azteca, (c) Figueira Branca and (d) Jauru models.

The magnetization, magnetic susceptibility and density obtained in each model of the Figueira Branca Suite (Fig. 10) agree with the context of gabbroic rocks intruded in a meta-volcanosedimentary environment described by geochemical (this work) and geological observations (D'Agrella-Filho et al., 2012; Teixeira et al., 2011). All cases presented similar values for magnetic susceptibility (Table 3), leaving the cause of the difference in the amplitude of the anomalies to the remanent magnetization. The shapes and depth extents can be associated with sills, as suggested by Teixeira et al. (2011). The layers of different lithologies could not be discriminated through the geophysical methods.

5. *Conclusions*

The Figueira Branca Suite is a layered mafic-ultramafic complex, dated at 1425 Ma, intruded into the Alto Jauru meta-volcanosedimentary group and adjacent to granites from the Santa Helena Orogen. Using magnetic field and gamma-ray geophysical data, we delineated the extent of the suite. Apart from the Indiavaí, Azteca, Figueira Branca and Jauru bodies, only two mafic intrusions in the northwest of the Jauru Terrane showed magnetic and gamma-ray signatures that could be related with the suite, however these two intrusions were recognized as the Morro do Leme and Morro do Sem-Boné complexes, part of the 1349 Ma Cacoal Suite. No other geophysical signatures similar to the four intrusions of the Figueira Branca Suite were found in the Jauru Terrane.

Thin sections of the Figueira Branca Suite indicated a mineralogy dominated by plagioclase, olivine and variable amounts of intergrown pyroxene (0 to 30%). This mineralogy indicates gabbroic rocks, as it was shown in the TAS. Magnetite is likely opaque minerals phase and is present in all samples. The increase in the amount of pyroxene among the samples from one intrusion to another in the Figueira Branca Suite suggests a fractionation in the parental magma. REE analyses normalized to chondrites showed a trend of major enrichment of LREE over HREE elements. The change in the slope of the REE normalized to chondrites indicates an increase in the amount of melt in the parental magma. These two changes suggest that the extraction of magma generated the bodies of the Figueira Branca Suite in the sequence: Indiavaí, Figueira Branca, Azteca and Jauru.

Magnetic and gravity fields were used to compose 3D models constrained by magnetic susceptibility (average of 0.06) and density (average of 2.93 g/cm³) measurements. This data combined with new field investigation and geochemical data indicate sill-like shapes extending 8 km on average in the northwest direction. The calculated remanent magnetizations are similar to the direction suggested by previously published paleomagnetic data of the Indiavaí gabbro.

Trace element concentrations suggested that the parental magma of the Figueira Branca Suite is associated with metasomatic processes of subduction zones. The magma was characterized by hydrous melts, typical from supra-subduction environments. The northwest alignment of the bodies, indicated by geological observation and geophysical modelling, is perpendicular to the direction of accretion of the terranes in southwest Amazon Craton and parallel to regional shear zones. The suite is located to east-northeast of the orogen and paleo-subduction zone that generated the Santa Helena orogen, marked by the Piratininga and Caramujo shear zones (Fig. 1).

Previously published isotope data show a juvenile mantle source for the Figueira Branca Suite. The integration of these data with those presented in this paper indicate that the magmatism that generated the Figueira Branca Suite during a phase of extension of the Jauru

Terrane. This event occurred during the late stages of emplacement of the Santa Helena orogeny (1425 Ma) and was interpreted as a magmatism in a back-arc setting.

6. Acknowledgements

We would like to thank Vanessa B. Ribeiro for the comments, and the Brazilian Geological Service for the data. This work was done with the support of the CNPq, National Council for Technological and Scientific Development – Brazil.

7. *References*

Bettencourt, J.S., Leite Jr, W.B., Ruiz, A.S., Matos, R., Payolla, B.L., Tosdal, R.M., 2010. The Rondonian-San Ignacio Province in the SW Amazonian Craton: An overview. Journal of South American Earth Sciences 29, 28-46.

Cordani, R., Shukowsky, W., 2009. Virtual Pole from Magnetic Anomaly (VPMA): A procedure to estimate the age of a rock from its magnetic anomaly only. J Appl Geophys 69, 96-102.

Cordani, U.G., Fraga, L.M., Reis, N., Tassinari, C.C.G., Brito-Neves, B.B., 2010. On the origin and tectonic significance of the intra-plate events of Grenvillian-type age in South America: A discussion. Journal of South American Earth Sciences 29, 143-159.

Corrêa da Costa, P.C., Girardi, V.A.V., Matos, J.B.d., Ruiz, A.S., 2009. Geocronologia Rb-Sr e características geoquímicas dos diques máficos da região de Nova Lacerda e Conquista D'Oeste (MT), porção sudoeste do Craton Amazônico [Rb-Sr geochronology and geochemical characteristics of mafic Dykes in the Nova Lacerda and Conquista D'Oeste region, Mato Grosso, SW Amazonian Craton]. Geologia USP: Série Científica 9, 17.

D'Agrella-Filho, M.S., Trindade, R.I.F., Elming, S.A., Teixeira, W., Yokoyama, E., Tohver, E., Geraldes, M.C., Pacca, I.I.G., Barros, M.A.S., Ruiz, A.S., 2012. The 1420 Ma Indiavai Mafic Intrusion (SW Amazonian Craton): Paleomagnetic results and implications for the Columbia supercontinent. Gondwana Res 22, 956-973.

Dickson, B.L., Scott, K.M., 1997. Interpretation of aerial gamma-ray surveys – adding the geochemical factors. AGSO Journal of Australia Geology and Geophysics 17, 13.

Fedi, M., Florio, G., Rapolla, A., 1994. A Method to Estimate the Total Magnetization Direction from a Distortion Analysis of Magnetic-Anomalies. Geophys Prospect 42, 261-274.

Foss, C., 2006. Evaluation of strategies to manage remanent magnetization effects in magnetic field inversion, 76th Annual SEG International Meeting. SEG, New Orleans, p. 4.

Geraldes, M.C., Van Schmus, W.R., Condie, K.C., Bell, S., Teixeira, W., Babinski, M., 2001. Proterozoic geologic evolution of the SW part of the Amazonian Craton in Mato Grosso state, Brazil. Precambrian Res 111, 91-128.

Girardi, V.A.V., da Costa, P.C.C., Teixeira, W., 2012. Petrology and Sr-Nd characteristics of the Nova Lacerda dike swarm, SW Amazonian Craton: new insights regarding its subcontinental mantle source and Mesoproterozoic geodynamics. Int Geol Rev 54, 165-182.

Kepezhinskas, P., McDermott, F., Defant, M.J., Hochstaedter, A., Drummond, M.S., Hawkesworth, C.J., Koloskov, A., Maury, R.C., Bellon, H., 1997. Trace element and Sr-Nd-Pb isotopic constraints on a three-component model of Kamchatka arc petrogenesis. Geochim Cosmochim Ac 61, 577-600.

Louro, V.H.A., Mantovani, M.S.M., Ribeiro, V.B., 2014. Magnetic field analysis of Morro do Leme nickel deposit. Geophysics 79, K1-K9.

Matos, J.B.d., Silva, C.H.d., Costa, A.C.D.d., Ruiz, A.S., Souza, M.Z.A.d., Batata, M.E.F., Corrêa da Costa, P.C., Paz, J.D.d.S., 2009. Geologia e Recursos Minerais da Folha Jauru (SD.21-Y-C-III), Programa Geologia do Brasil, Cuiabá, p. 134.

Mcdonough, W.F., Sun, S.S., 1995. The Composition of the Earth. Chem Geol 120, 223-253.

Menezes, R.G., 1993. Pontes e Lacerda. Folha SD. 21-Y-c-n, Programa Levantamentos Geológicos Básicos do Brasil - PLGB. CPRM - Serviço Geológico do Brasil.

Middlemost, E.A.K., 1994. Naming Materials in the Magma Igneous Rock System. Earth-Sci Rev 37, 215-224.

Nunes, N.S.d.V., 2000a. Geologia e resultados prospectivos da área de Figueira Branca/Indiavaí, Mato Grosso, Série Metais do Grupo da Platina e Associados, 24 ed. CPRM - Serviço Geológico do Brasil.

Nunes, N.S.d.V., 2000b. Geologia e resultados prospectivos das áreas Morro do Leme e Morro Sem Boné/Mato Grosso, Série Metais do Grupo da Platina e Associados, CPRM - Serviço Geológico do Brasil ed. CPRM - Serviço Geológico do Brasil, Goiânia, p. 61.

Quadros, N.L.E.S., Rizzotto, G.J., 2007. Geologia e recursos minerais do Estado de Rondônia: Sistema de Informações Geográficas – SIG: Texto Explicativo do Mapa Geológico e de Recursos Minerais do Estado de Rondônia., Programa Geologia do Brasil. CPRM, Porto Velho, p. 153 p.

Rizzotto, G.J., Santos, J.O.S., Hartmann, L.A., Tohver, E., Pimentel, M.M., McNaughton, N.J., 2013. The Mesoproterozoic Guapore suture in the SW Amazonian Craton: Geotectonic implications based on field geology, zircon geochronology and Nd-Sr isotope geochemistry. Journal of South American Earth Sciences 48, 271-295.

Roest, W.R., Verhoef, J., Pilkington, M., 1992. Magnetic Interpretation Using the 3-D Analytic Signal. Geophysics 57, 116-125.

Ruiz, A.S., 2005. Evolução Geológica do Sudoeste do Cráton Amazônico Região Limítrofe Brasil-Bolívia-Mato Grosso, Departamento de Geociências. UNESP - Rio Claro, Rio Claro, p. 299.

Saes, G.S., Leite, J.A.S., Weska, R.K., 1984. Geologia da Folha Jauru (SD.21.Y.C.III): uma síntese de conhecimentos, 33rd Congresso Brasileiro de Geologia. Sociedade Brasileira de Geologia, Rio de Janeiro.

Shervais, J.W., 1982. Ti-V Plots and the Petrogenesis of Modern and Ophiolitic Lavas. Earth Planet Sc Lett 59, 101-118.

Souza, M.Z.A.d., Batata, M.E.F., Ruiz, A.S., Lima, G.A.d., Matos, J.B.d., Paz, J.D.d.S., Costa, A.C.D.d., Silva, C.H.d., Corrêa da Costa, P.C., 2009. Geologia e Recursos Minerais da Folha Rio Branco (SD-21-Y-D-1), Programa Geologia do Brasil, Cuiabá, p. 178.

Sun, S.-s., McDonough, W.F., 1989. Chemical and isotopic systematics of oceanic basalts: implications for mantle composition and processes. Geological Society, London, Special Publications 42, 313-345.

Tassinari, C.C.G., Bettencourt, J.S., Geraldes, M.C., Macambira, M.J.B., Lafon, J.M., 2000. The Amazonian Craton, in: Cordani, U.G., Milani, E.J., Thomaz Filho, A., Campos, D.A. (Eds.), 31st International Geological Congress. Sociedade Brasileira de Geologia, Rio de Janeiro, pp. 41-95.

Tassinari, C.C.G., Macambira, M.J.B., 1999. Geochronological provinces of the Amazonian Craton. Episodes 22, 174-182.

Teixeira, W., Ernst, R.E., Hamilton, M.A., Lima, G., Ruiz, A.S., Geraldes, M.C., 2016. Widespread ca. 1.4 Ga intraplate magmatism and tectonics in a growing Amazonia. Gff 138, 241-254.

Teixeira, W., Geraldes, M.C., D'Agrella, M.S., Santos, J.O.S., Barros, M.A.S., Ruiz, A.S., da Costa, P.C.C., 2011. Mesoproterozoic juvenile mafic-ultramafic magmatism in the SW Amazonian Craton (Rio Negro-Juruena province): SHRIMP U-Pb geochronology and Nd-Sr constraints of the Figueira Branca Suite. Journal of South American Earth Sciences 32, 309-323.

Teixeira, W., Geraldes, M.C., Matos, R., Ruiz, A.S., Saes, G., Vargas-Mattos, G., 2010. A review of the tectonic evolution of the Sunsas belt, SW Amazonian Craton. Journal of South American Earth Sciences 29, 47-60.

Vermeesch, P., 2006. Tectonic discrimination diagrams revisited. Geochemistry, Geophysics, Geosystems 7, n/a-n/a.

Wang, H., Wu, Y.B., Qin, Z.W., Zhu, L.Q., Liu, Q., Liu, X.C., Gao, S., Wijbrans, J.R., Zhou, L., Gong, H.J., Yuan, H.L., 2013. Age and geochemistry of Silurian gabbroic rocks in the Tongbai orogen, central China: Implications for the geodynamic evolution of the North Qinling arc-back-arc system. Lithos 179, 1-15.

Zheng, Y.F., 2012. Metamorphic chemical geodynamics in continental subduction zones. Chem Geol 328, 5-48.

Tectonic insights of the Southwest Amazon Craton from geophysical, geochemical and mineralogical data of Figueira Branca Mafic-Ultramafic Suite, Brazil

Vinicius Hector Abud Louro, Peter Anthony Cawood, Marta Silvia Maria Mantovani

Graphical Abstract

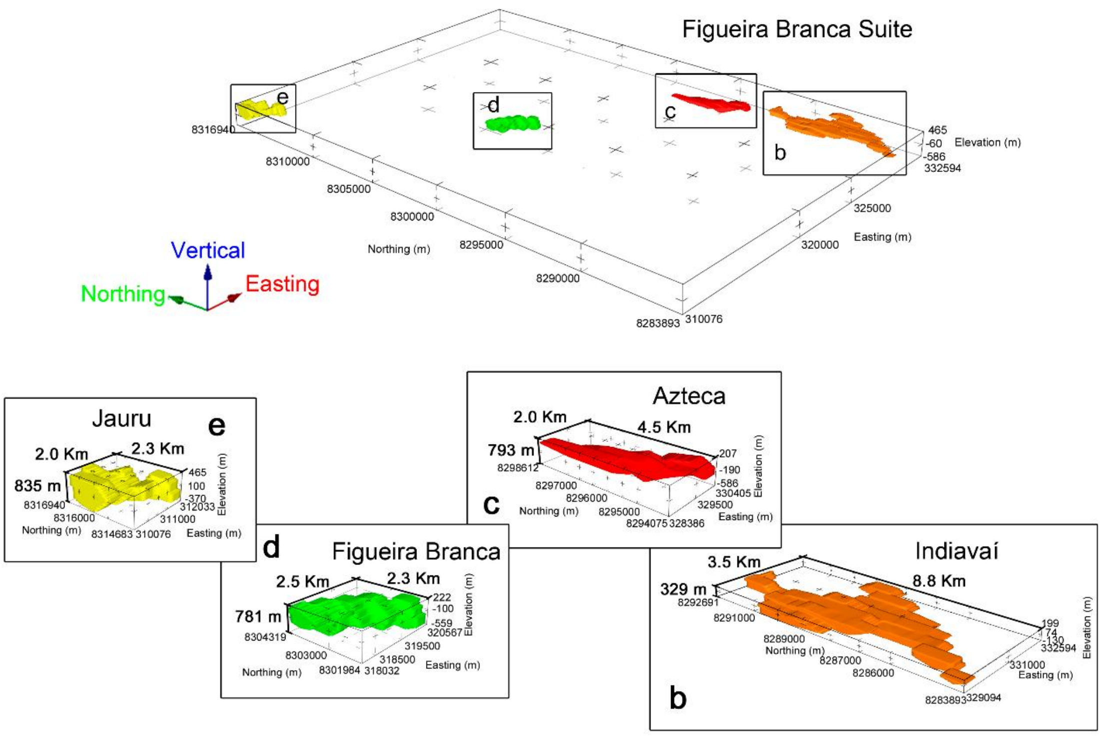

Joint magnetic and gravity models of the Figueira Branca Suite constrained by petrophysical, geochemical and mineralogical analysis. In detail, (a) Indiavaí, (b) Azteca, (c) Figueira Branca and (d) Jauru models.

Tectonic insights of the Southwest Amazon Craton from geophysical, geochemical and mineralogical data of Figueira Branca Mafic-Ultramafic Suite, Brazil

Vinicius Hector Abud Louro, Peter Anthony Cawood, Marta Silvia Maria Mantovani

Highlights

- A model for the tectonic framework of the Jauru Terrane at 1.42 Ga is proposed.
- Gravity and magnetic field models constrained by geochemistry and mineralogy.
- The multi-method data showed indicated mafic intrusions in a back-arc setting.